Journal of Magnetic Resonance **143,** 233–239 (2000)
doi:10.1006/jmre.2000.2016, available online at http://www.idealibrary.com on IDEAL®

^{1}H Dynamic Nuclear Polarization in Supercritical Ethylene at 1.4 T

Robert A. Wind,*[,1] Shi Bai,*[,2] Jian Z. Hu,† Mark S. Solum,† Paul D. Ellis,* David M. Grant,† Ronald J. Pugmire,‡ Craig M. V. Taylor,§ and Clement R. Yonker*

*Pacific Northwest National Laboratory, P.O. Box 999, Richland, Washington 99352; †Department of Chemistry and ‡Department of Chemical and Fuels Engineering, University of Utah, Salt Lake City, Utah 84112; and §Los Alamos National Laboratory, Los Alamos, New Mexico 87545

Received September 8, 1999; revised January 5, 2000

^{1}H dynamic nuclear polarization (DNP) has been measured in supercritical ethylene in the pressure range 60–300 bar in an external field of 1.4 T. A single-cell sapphire tube was used as a high-pressure cell, and powdered 1,3-bisdiphenylene-2-phenyl allyl (BDPA) free radicals were added and distributed at the wall of the cell. At all pressures the dominant DNP mechanism was a positive Overhauser enhancement, caused by proton–electron contact interactions at the fluid/solid radical interface. The observed enhancements varied from 12 at 60 bar to 17 at 300 bar. Besides the Overhauser enhancement, small solid state and thermal mixing enhancements also were observed, indicating that part of the ethylene was adsorbed at the radical surface for a prolonged time. The impacts of the experimental conditions on the Overhauser enhancement factors are discussed, and enhancements of at least 40–60 are estimated when the EPR saturation factor and the leakage factor become maximal. These data indicate that DNP-enhanced NMR has the potential of extending the impact of NMR in research areas involving supercritical fluids. © 2000 Academic Press

Key Words: **DNP; Overhauser effect; supercritical fluids; ethylene.**

INTRODUCTION

Supercritical fluids (SCFs) have both liquid and gas phase properties, such a high density, giving it appreciable solvating power, and a low viscosity, facilitating mass transport of solutes in the SCFs. Moreover, these parameters can be varied over a relatively large range by adjusting the temperature and/or the pressure. These properties, together with the benefit that many SCFs such as carbon dioxide or water are safe and nonhazardous when depressurized, has triggered the use of SCFs in a large variety of industrial processes such as extraction, separation, catalysis, cleaning, and polymerization (*1–8*).

All these unique properties of SCFs and their environmentally significant applications make it important to understand these fluids as well as the processes involving SCFs in detail. NMR has been used to investigate the properties of SCFs (*9*), but the relatively low sensitivity of the technique limits its utility to high solute concentrations. Therefore, it is important to develop methodologies that increase NMR sensitivity in SCFs. One of the techniques which has the potential to produce large enhancements of the NMR signal in SCFs is dynamic nuclear polarization (DNP), and in this communication we report the first DNP results obtained in supercritical ethylene.

DYNAMIC NUCLEAR POLARIZATION

Extensive reviews of the DNP phenomenon have been published elsewhere (*10–21*). DNP can be applied to materials containing both magnetic nuclei and unpaired electrons. A polarization transfer between the two spin systems can be achieved by irradiating at or near the electron Larmor frequency ω_e, resulting in enhanced nuclear polarization. Several mechanisms can contribute to the DNP effect, depending on the type and time dependence of the electron–nuclear interactions governing the polarization transfer. In solids, where the interactions often have a nonzero static component, the DNP enhancement arises from the so-called solid state and thermal mixing effects. In both cases the enhancement curve, i.e., the nuclear signal enhancement factor as a function of the irradiation frequency, is anti-symmetric about ω_e. In liquids the molecular motions render the electron–nuclear interactions time-dependent, and the polarization transfer is governed by the Overhauser effect (*22*). The enhancement curve, which reflects the (saturated) EPR line, is often symmetric about ω_e. Theory suggests that large signal enhancements can be achieved with maximum enhancement factors bounded by the ratio of the gyromagnetic ratios of the electron and the target nucleus, e.g., 660 for protons, 2600 for ^{13}C, and 6500 for ^{15}N. In practice the theoretical maximum enhancement factors are often reduced for a variety of reasons, but enhancement factors of 1–2 orders of magnitude have been observed, and it is obvious that DNP has the potential for increasing the NMR sensitivity significantly.

In case the EPR spectrum consists of a single line, the Overhauser enhancement E_{OV} is given by (*12, 14, 16, 18, 20*)

$$E_{OV} = 1 - \rho f s |\gamma_e| / \gamma_n. \quad [1]$$

[1] To whom correspondence should be addressed. E-mail: robert.wind@pnl.gov.

[2] Current address: Department of Chemistry and Biochemistry, University of Delaware, Delaware 19716.

1090-7807/00 $35.00

The parameter f is the leakage factor, given by $f = 1 - T_1/T_{10}$, where T_1 and T_{10} are the nuclear spin-lattice relaxation times in the presence and absence of the radicals, respectively; s is the saturation factor, given by $s = 1 - P_e/P_{eo}$, where P_e and P_{eo} are the electron polarizations in the presence and absence of the irradiation field, respectively; and γ_e and γ_n are the electron and nuclear gyromagnetic ratios. The maximum values of f and s are unity. Furthermore, the parameter ρ in Eq. [1] is the coupling factor, determined by the strengths of the electron–nuclear dipolar and scalar interactions and by the spectral density functions $J_D(\omega)$ and $J_s(\omega)$ characterizing the time dependence in these interactions. Using the fact that the electron Larmor frequency ω_e is much larger than the nuclear Larmor frequency ω_n, the coupling factor can be written as (*14, 16*)

$$\rho = \{f_D(\omega_e\tau_{cD}) - Kf_s(\omega_e\tau_{cs})\}/ \{1.4f_D(\omega_e\tau_{cD}) + 0.6f_D(\omega_n\tau_{cD}) + Kf_s(\omega_e\tau_{cs})\}, \quad [2]$$

$f_D(\omega\tau_{cD}) = J_D(\omega\tau_{cD})/J_D(\omega = 0)$ and $f_s(\omega\tau_{cs}) = J_s(\omega\tau_{cs})/J_s(\omega = 0)$ are the reduced spectral density functions associated with the dipolar and scalar interactions, respectively, and K describes the magnitude of the scalar interactions relative to the dipolar interactions. The parameters τ_{cD} and τ_{cs} are the correlation times characterizing the time dependence in the dipolar and scalar interactions, respectively.

It follows from Eq. [1] that the value of ρ that can be obtained depends on both the relative strengths of the dipolar and scalar interactions and the corresponding spectral density functions. In the extreme narrowing case, where $\omega\tau_{cD}$, $\omega\tau_{cs} \ll 1$, ρ varies between -1 for pure scalar interactions and $+\frac{1}{2}$ for pure dipolar interactions. Hence for nuclei with a positive γ_n value the maximum value of $E_{OV} - 1$ varies between $+|\gamma_e|/\gamma_n$ and $-0.5|\gamma_e|/\gamma_n$. The spectral density functions depend on the details of the molecular motions that render the electron–nuclear interactions time dependent. Examples of such motions are the translational and rotational diffusion of the liquid molecules, rotations of possible liquid–radical complexes, inelastic and elastic collisions between the liquid and radical molecules, and, in case nondissolved solid radicals are used, exchange effects on the liquid/solid interfaces (*12, 14, 16, 23–26*). Which of these motions dominates in the coupling factor depends on the electron Larmor frequency ω_e and, henceforth, on the value of the external field. At low frequencies, where $\omega_e\tau_{cD}$, $\omega_e\tau_{cs} \ll 1$, ρ is dominated by the relatively slow motions associated with the translational diffusion, exchange effects, and inelastic collisions, whereas at larger frequencies faster processes such as rotational diffusion and elastic collisions play an increasingly important role (*12, 14, 16*). The coupling factor decreases more or less rapidly at larger frequencies, where the extreme narrowing condition is no longer valid. Under these conditions the dipolar spectral density function $f_D(\omega_n\tau_{cD})$ becomes the dominant term in Eq. [2]. This is important because the DNP-enhanced NMR polarization is proportional to $|E_{OV}|M_o$, where M_o is the thermal equilibrium magnetization. Therefore, in order to obtain the maximum DNP-enhanced NMR sensitivity, the external field B_o should be as large as possible. However, the frequency dependence of ρ limits the value of the field. In liquids τ_c is typically of the order of 10–100 psec at room temperature (*14, 16*), and the enhancements decrease rapidly for fields above 0.03–0.3 T. However, in supercritical fluids the diffusion coefficients can be more than an order of magnitude larger than in ordinary liquids (*27*). Hence the correlation times associated with these motions are reduced by the same factor, and the same is probably true for the correlation times characterizing the elastic and inelastic collisions, as it has been found that in liquids these correlation times are proportional to the translational diffusion time (*14*). Therefore it can be expected that in supercritical fluids even in relatively large fields appreciable DNP enhancements can be obtained, and it will be demonstrated in this communication that this is indeed the case.

Two methods can be used to introduce unpaired electrons into a SCF. First, if a suitable free radical will dissolve in the SCF, then all SCF nuclei experience the same electron–nuclear interactions and a homogeneous enhancement occurs. This approach has been used by Dorn and co-workers (*28*), who measured a proton Overhauser enhancement of -140 for benzene dissolved in supercritical CO_2, doped with a nitroxide radical (and this enhancement is estimated to become at least -260 for $s = f = 1$). Second, solid free radicals can be used which will not dissolve in the SCF or are immobilized in a solid matrix (*29, 30*). This method has the advantage that the radicals do not contaminate the SCF, which prevents possible alterations of chemical processes involving SCFs. Moreover, it facilitates the transport of the polarized SCF molecules to areas outside the microwave region, as the relaxation times of the nuclei in these molecules are no longer shortened by the radicals. In liquids this approach has been used by Odintsov *et al.* (*24–26*) for a low-field DNP investigation on aqueous char suspensions, and by Dorn *et al.* (*29, 30*) to perform NMR spectroscopy at a larger field than that used for DNP. When the radicals are present as a solid, DNP is governed by interactions between the SCF nuclei and the unpaired electrons at or near the solid/fluid interface, rendered time-dependent by molecular motions similar to those of dissolved radicals. Henceforth the DNP enhancement of the nuclei close to the radicals should be similar to that in the case of dissolved radicals, provided that the strengths of the various interactions are the same in both cases.

In this communication the second approach has been used. ^{1}H DNP results are reported in supercritical ethylene in the presence of the powdered form of the stable free radical 1,3-bisdiphenylene-2-phenyl allyl (BDPA), obtained from Aldrich. This free radical is essentially insoluble in ethylene. Ethylene was chosen mainly because of its strong ^{1}H NMR signal and low critical temperature and pressure (282.4 K and 50.4 bar,

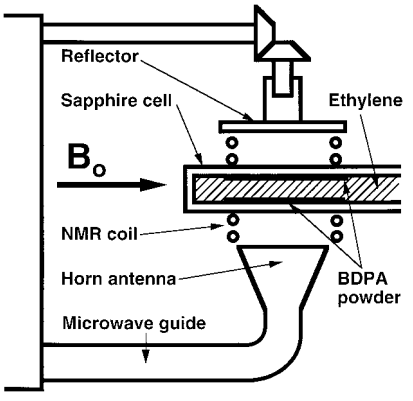

FIG. 1. Sketch of the DNP/NMR probe. The reflector can be moved forward and backward relative to the horn antenna via a rotating gear and a screw-type mechanism. In this way the microwave field at the location of the sample can be maximized.

respectively), which enabled us to carry out experiments at ambient temperatures and relatively low pressures.

EXPERIMENTAL

The DNP-NMR spectrometer employed in this study was developed and placed at the University of Utah. It operates at a field of 1.4 T, corresponding to electron and ^{1}H Larmor frequencies of 40 GHz and 60 MHz, respectively. The spectrometer utilizes a Chemagnetics CMX-100 console and a horizontal magnet from Magnex, with a clear bore size of 22 cm. Microwave irradiation is achieved with a Wiltron microwave frequency synthesizer, model 68263B, and a 10 W c.w. Traveling Wave Tube amplifier (Logimetrics model A400/KA). Figure 1 shows a sketch of the DNP-NMR probe used in the experiments. The probe is home-built, and is capable of performing DNP-NMR on static samples with volumes up to 0.5 ml. This setup is a variant of previous designs (*17, 18*). The microwave irradiation is obtained using a combination of a cylindrical horn antenna with a diameter of 10 mm and a moveable reflector. The NMR coil has the same diameter as the horn opening, and is placed with its axis coincident with that of the horn antenna. In this way shielding of the microwaves by the NMR coil is avoided (*31*). With this design it is estimated that the 10 W incident microwave power produces a microwave field in the sample of about 0.04 mT (rotating component). The probe is equipped with two modulation coils, connected (via a home-built power amplifier) to a SR850 DSP lock-in amplifier from Stanford Research Systems. This, in combination with the microwave frequency sweep, makes it possible to perform c.w. first-derivative 40 GHz EPR.

For DNP-NMR measurements on SCFs, high-pressure cells such as fused silica capillary tubing (*32*) or single-crystal sapphire tubes (*33*), which are transparent for the microwaves, need to be employed. In the experiments reported in this communication a single-crystal sapphire tube was used (Saphpicon, Inc., Milford, NH) with an OD of 5 mm and a wall thickness of 1.5 mm, glued into a titanium holder, which is connected to a high-pressure pump (ISCO Model 260D syringe pump) via a 1/16-in. stainless steel capillary (*33*). The sapphire cell can support pressures up to 600 bar at room temperature, well above the critical pressure of ethylene. As the length of the cell exceeds the available distance between the horn opening and the reflector, it was mounted with its axis perpendicular to that of the NMR coil by inserting it into a 5-mm gap in the middle of the coil (see Fig. 1). A disadvantage of this setup is that the filling factor of the coil is rather small, which reduces the NMR sensitivity. This situation can be improved considerably by using a saddle coil mounted around the pressure cell. However, this approach was not pursued for the initial DNP measurements, because this would have required a major redesign of the probe layout, and because with the used configuration the NMR sensitivity was sufficiently large to measure the DNP enhancement factors accurately.

For the DNP experiments about 4 mg of powdered BDPA was placed in the sapphire tube and, by shaking the tube, most of the powder was displaced into the DNP/NMR area of the tube. The cell was inserted into the DNP probe, connected to the high pressure pump, and flushed several times with ethylene gas before the ethylene was pressurized. From a visual inspection of the sample in the pressurized tube it was concluded that little if any of the BDPA is dissolved in the ethylene (based on the lack of any discoloration of the liquid) when the pressure is below 100 bar, and that most of the powder was attached to the wall of the sapphire tube. When the pressure exceeds 100 bar the SCF slowly becomes slightly colored as the solubility of the BDPA increases with pressure. Further, BDPA particles were not observed to be suspended in the SCF, probably a result of the low ethylene density (*34*).

Despite the rather rudimentary experimental setup the reproducibility of the results is reasonable. In duplicate experiments the maximum DNP enhancements varied by approximately 30% (probably resulting from varying amounts of BDPA in the DNP/NMR region of the tube), but the trends in the enhancement factors as a function of pressure were very similar. All measurements were performed at room temperature.

RESULTS AND DISCUSSION

EPR

Figure 2 shows the 40 GHz EPR spectrum of BDPA in absence of the ethylene. A single line with a width of 4.8 MHz (FWHM), which is slightly asymmetric as a result of an anisotropy in the g-factor, is observed. Similar spectra were obtained in the presence of ethylene at all pressures considered, which is another indication that the BDPA radical is not dissolving into the ethylene. The narrow linewidth is the same as that observed in pure BDPA and is a result of electron–

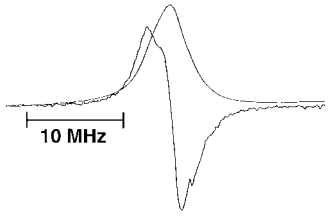

FIG. 2. EPR first derivative spectrum and its integral of BDPA observed at 40 GHz.

electron spin exchange narrowing, which becomes significant when the concentration of unpaired electrons is high (*10*, *35*).

^{1}H NMR

In Fig. 3 the proton spectrum of supercritical ethylene with BDPA introduced into the cell is compared with a sample in which no free radical was present. Despite the rather broad lines due to the limited shimming capabilities of the magnet, it can be seen that the presence of BDPA induces two more peaks into the ethylene spectrum, located at 6.9 and 3.7 ppm. These new resonance frequencies are probably caused by local field inhomogeneities created by the presence of the solid BDPA in the sapphire tube. Although both the T_1 values and the maximum DNP enhancement factors differ by about 10–30% for the different peaks, the poor spectral resolution prevents proper determination of these parameters for the individual lines. In the following paragraph, only average values obtained from the integrated line intensities will be discussed.

^{1}H DNP

Figures 4A and 4B show the enhancement curve, i.e., the DNP enhancement factor minus unity, $E - 1$, as a function of the microwave frequency, obtained at 200 bar. A relatively

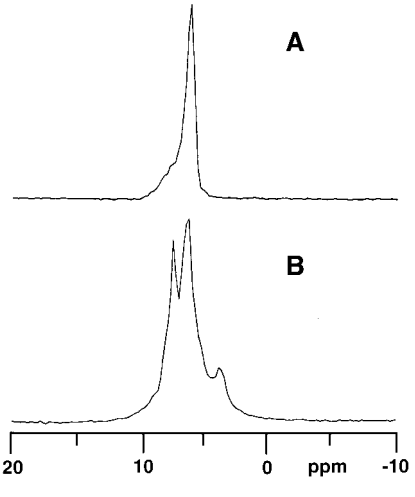

FIG. 3. Proton spectra of supercritical ethylene obtained at 60 bar and 26°C (A) without BDPA; (B) in the presence of BDPA. Both spectra were obtained with four scans.

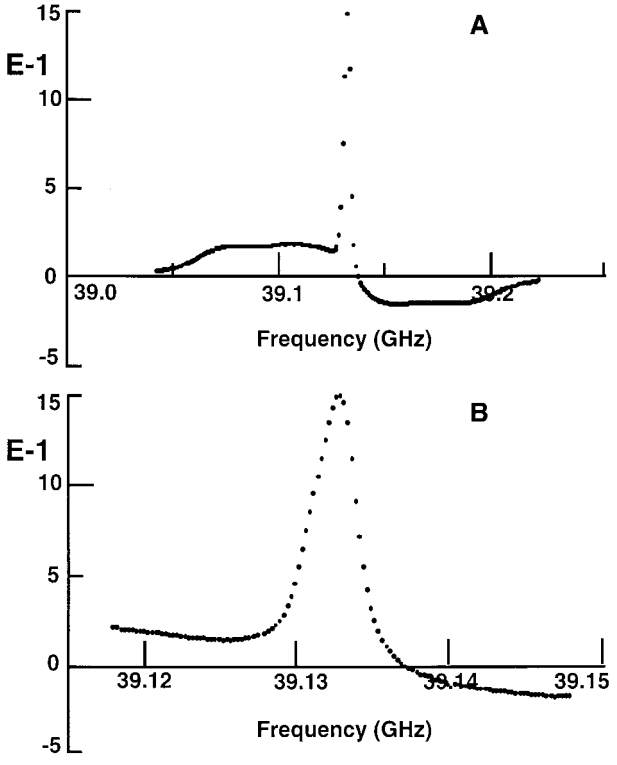

FIG. 4. The ^{1}H DNP enhancement curve obtained on supercritical ethylene at 200 bar and 26°C. (A) the full enhancement curve; (B) the Overhauser part of the enhancement curve.

large and positive Overhauser enhancement is measured, indicating that the positive enhancement due to proton–electron scalar interactions dominates the negative enhancement resulting from the dipolar interactions. This is unusual for proton DNP, where scalar interactions can usually be neglected (*20*). However, this observation is consistent with recent DNP measurements of water protons in an aqueous suspension of a hardwood char, where positive Overhauser enhancements were observed by Odintsov *et al.* on the sample at temperatures above 315 K (*24–26*). Figure 4B shows the Overhauser part of the enhancement curve, which reflects the saturated EPR spectrum. The width of this curve is about 3.5 MHz, which is smaller than that of the unsaturated EPR line, cf. Fig. 2. Hence the EPR line becomes narrower under saturation, which occurs in solid materials when the spin-lattice relaxation time of the electron dipolar system is comparable to the electron Zeeman relaxation time (*13*).

It follows from Fig. 4A that a component of the enhancement curve is anti-symmetrical about the electron Larmor frequency, with maxima and minima observed in the frequency range corresponding to the solid state and thermal mixing conditions. This observation indicates that part of the ethylene is adsorbed at the surface for a time long compared to the inverse of electron–nuclear dipolar coupling strengths, resulting in a nonzero static component (a similar result was observed in water adsorbed on sucrose chars (*36*)). It is worth

TABLE 1

The ^{1}H DNP Enhancement Factor and the Longitudinal Relaxation Times of Supercritical Ethylene Measured at 60, 200, and 300 Bar

Pressure (bar)	E_{OV} exp	T_1 (sec)	$(T_{1o})_A$ (sec)	f	$(E_{OV})_o$ $s = f = 1$	$(T_{1o})_B$ (sec)
60	11.9	8.3	13	0.36	55	25
200	15.8	9.0	25	0.64	41	29
300	17.1	8.3	22	0.62	46	32

Note. E_{OV} is the Overhauser enhancement of the integrated signal, observed with an incident microwave power of 10 W; T_1 is the relaxation time of ethylene in the presence of BDPA; $(T_{1o})_A$ is the relaxation time of ethylene in the absence of BDPA; f is the leakage factor, given by $f = 1 - T_1/(T_{1o})_A$; $(E_{OV})_o$ is the Overhauser enhancement calculated for $f = s = 1$, using $s = 0.6$ at maximum power; $(T_{1o})_B$ is the relaxation time in the absence of BDPA in the sapphire tube with the plug inserted into the tube.

noting that the shape of the anti-symmetrical part of the enhancement curve at (absolute) microwave offset frequencies larger than 60 MHz (the proton Larmor frequency) reflects one-half of the unsaturated EPR line of the unpaired electrons contributing to the solid state effect (*18, 19*). It can be determined from Fig. 4 that the width of this line is about 28 MHz (FWHM), considerably larger than the measured EPR linewidth of 4.8 MHz. Apparently for the fraction of the unpaired electrons responsible for the solid state and thermal mixing enhancements the electron–electron spin-exchange interactions are quenched, perhaps as a result of a decreased delocalization in the electron density when an ethylene molecule is adsorbed on a BDPA molecule. Within the uncertainty imposed by the signal-to-noise ratio this broad component was not observed in the EPR measurement, indicating that the fraction of unpaired electrons possessing this lineshape is small.

Table 1 gives Overhauser enhancement factors measured at 60, 200, and 300 bar. At all pressures the Overhauser effect is positive, which means that the scalar proton–electron interactions dominate the DNP mechanism. Substantial enhancements of 12–17 are observed, slightly increasing at higher pressures. It is also worth noting that at 45 bar, where the ethylene is in the gas phase, a positive enhancement of 13 was measured.

In order to determine the maximum Overhauser enhancement that can be expected in our present setup, both the saturation factor s and the leakage factor f must be known, cf. Eq. [1]. The saturation factor s was determined by measuring $1/(E_{OV} - 1)$ as a function of $1/P$, where P is the microwave power. A linear correlation between $1/(E_{OV} - 1)$ and $1/P$ was found. By extrapolating the curve to infinite microwave power, a maximum DNP enhancement factor, $(E_{OV} - 1)_\infty$, was obtained, and s is given by $s = (E_{OV} - 1)_{max}/(E_{OV} - 1)_\infty$, where $(E_{OV} - 1)_{max}$ denotes the DNP enhancement at maximum available microwave power. A value of $s = 0.6 \pm 0.1$ was determined. In order to determine the leakage factor, the T_1 values of ethylene in the presence and absence of the BDPA were measured, using the saturation recovery method. It was observed that the relaxation in the presence of BDPA was slightly nonexponential, which is presumably a result of the heterogeneous distribution of the BDPA in the sample. For simplicity the T_1 values were estimated from $T_1 = t_{1/2}/\ln 2$, where $t_{1/2}$ is the time it takes for the magnetization to reach half its thermal equilibrium value. The T_1 values and the leakage factors are given in Table 1, where also the Overhauser enhancements are given for $s = f = 1$. It follows that enhancements of 40–55 can be expected if s and f can be increased.

Several unknowns make it impossible in the present stage of the investigations to further analyze the results in a quantitative way: (i) the factor K in Eq. [2], which determines the relative contribution of the negative Overhauser enhancement due to electron–nuclear dipolar interactions and the positive enhancement due to the scalar interactions; (ii) the correlation times and the spectral density functions governing the various terms in Eq. [2]; and (iii) the fraction of ethylene molecules interacting with the unpaired electrons at the BDPA surface. Therefore we confine ourselves to remarking that the ultimate enhancements of 40–55 that can be expected in the relatively large field of 1.4 T are rather impressive, given that the actual enhancement due to the scalar interactions only may be considerably larger than observed, as it is in part compensated for by the negative enhancement arising from the dipolar interactions. Moreover, the measured overall DNP enhancement is probably reduced because only part of the ethylene is interacting with the BDPA, see below. Therefore the results can be regarded as a strong indicator that indeed the fast molecular motions in supercritical fluids result in large Overhauser enhancements, even in larger external fields. This also follows from a comparison of our results with DNP results obtained in liquids: For the DNP measurements on the aqueous char suspensions, which were performed in a low field (11.7 mT) (*24–26*), enhancement factors similar to those reported here were found on SCFs at 1.4 T. Moreover, although for radicals dissolved in organic liquids proton Overhauser enhancements have been observed at 1.4 T similar to those given here (*12, 14, 16*), it should be noted that in these cases possible enhancement reductions due to competing scalar and dipolar interactions and/or small fractions of interacting nuclei do not play a role.

CONCLUSIONS

It has been shown that it is possible to enhance the NMR signals of supercritical fluids substantially with the DNP technique, even in (for DNP) a relatively large field of 1.4 T. Therefore, this technique has significant potential for studying catalytic and other chemical processes utilizing these fluids. Moreover, by inserting gradient coils into the probe, DNP-NMR might also be used to improve measurements of the flow and diffusion properties of a SCF. Such experiments could be

used to study the penetration of SCFs in porous media and to image the distribution of SCFs in such media with an enhanced spatial resolution.

Although the initial results reported in this communication are encouraging, it should be emphasized that the obtained enhancement factors should be regarded as minimum values and that several improvements of the experimental setup are possible which may further increase the observed enhancement factors: (1) The saturation factor s can be increased by enhancing the microwave field amplitude, e.g., by positioning the horn antenna and the reflector closer to the sapphire tube. This can be realized by employing a saddle coil around the sample, which should also increase the filling factor and, henceforth, the NMR sensitivity. (2) The leakage factor f can be increased by enhancing the amount of ethylene molecules at the BDPA surface area. This can be achieved, e.g., by flowing the ethylene through a tube stacked with BDPA. (3) The coupling factor can be increased by flowing the ethylene in a controlled way over the BDPA. In this way the flow can be optimized for maximum electron–proton contact interactions, and this approach has the additional advantage that the DNP experiment can be separated from the NMR measurements. This can be achieved by pumping the SCF from the DNP area into the NMR coil, which can be located outside the microwave device used for DNP. In this way both the DNP and NMR setups can be optimized separately, and it also provides the possibility of performing NMR spectroscopy at a higher field than the DNP experiments, which further increases the NMR sensitivity as well as the spectral resolution (*29*, *30*). (4) The radicals can be immobilized in a solid matrix, e.g., by embedding the radicals in a solid such as silica gel (*30*). This eliminates a possible negative Overhauser enhancement due to dissolved radicals, which counteract the positive enhancement occurring at the fluid/solid interface. (5) The molecular exchange at the boundaries of the DNP/NMR region can be decreased. Due to the thermal motions an exchange occurs between the ethylene molecules containing polarized protons with the unpolarized molecules outside the microwave area and the NMR coil (*33*), which decreases the apparent observed Overhauser enhancement factors. That this effect cannot be neglected is illustrated by the T_1 values obtained when a plug was used to confine the ethylene to the sample area. These values are also given in Table 1, and it follows that without the plug the molecular exchange results in a considerable shortening of the apparent T_1 values. The DNP enhancement factors were also measured when a plug was inserted into the sapphire tube. However, in contrast to expectations it was found that with this plug in place the Overhauser enhancement was reduced by almost an order of magnitude. This indicates that without the plug macroscopic motions such as thermal convection resulting from, e.g., small temperature gradients probably occur, which increases the exchange of ethylene at the surface with the surrounding ethylene. This exchange increases the fraction of ethylene interaction with the BDPA, resulting in an increased overall DNP enhancement. This problem can be solved using a flow system, where the ethylene is transported through a tube with stacked, immobilized BDPA and placed within the microwave region in a confined area surrounded by the NMR coil.

It is worth noting that these improvements will make it possible to improve the quantitative analysis of the DNP results as well. However, for a complete analysis more parameters need to be measured, namely the factor K in Eq. [2], determining the relative strengths of the dipolar and scalar interactions and the various spectral density functions occurring in Eq. [2]. K can be obtained from low-field DNP measurements, where the various reduced spectral density functions occurring in Eq. [2] can be approximated by unity; and the spectral density functions can be determined by performing DNP experiments in a variety of external fields.

Future investigations will focus on implementing the instrumental improvements mentioned above. This setup will be used to perform comprehensive studies of the temperature and pressure dependence of the DNP enhancements in supercritical fluids, using both immobilized radicals and radicals that will dissolve in the SCF. For these studies also the use of fused silica capillaries as a pressure cell will be explored (*32*), which will make it possible to study DNP SCFs with larger critical pressures and over a larger pressure range than is possible with the sapphire crystals.

ACKNOWLEDGMENTS

Support for R. Wind's participation in the project was provided by the Pacific Northwest National Laboratory, a multiprogram laboratory operated by Battelle Memorial Institute for the U. S. Department of Energy under Contract DE-AC06_76RLO 1830. Support for the work at the University of Utah was provided by the Japanese government (New Energy Development Organization), the Department of Energy under Contract DE-FG-02-94ER14452 from the Division of Chemical Sciences of the Office of Basic Energy Sciences, the Los Alamos National Laboratory under Subcontract E90240017-23, the University of Utah, and the Pacific Northwest National Laboratory under Subcontract 353465-A-5E.

REFERENCES

1. T. G. Squires and M. E. Paulatis, Eds., "Supercritical Fluids," ACS Symposium Series, Vol. 329, Am. Chem. Soc., Washington, DC (1987).
2. R. W. Shaw, T. B. Brill, A. A. Clifford, C. A. Eckert, and E. U. Frank, Supercritical water: A medium for chemistry, *Chem. Eng. News* **69,** 26–39 (1991).
3. T. W. Randolph and C. Carlier, Free-radical reactions in supercritical ethane: A probe of supercritical fluid structure, *J. Phys. Chem.* **96,** 5146–5151 (1992).
4. K. W. Hutchenson and N. R. Foster, Eds., "Innovations in Supercritical Fluids," ACS Symposium Series, Vol. 608, Am. Chem. Soc., Washington, DC (1995).
5. P. G. Jessop, T. Ikariya, and R. Noyori, Homogeneous catalysis in supercritical fluids, *Science* **269,** 1065–1069 (1995).
6. C. A. Eckert, B. L. Knutson, and P. G. Debenetti, Supercritical fluids

as solvents for chemical and materials processing, *Nature* **383,** 313–318 (1996).

7. L. T. Taylor, "Supercritical Fluid Extraction," Wiley, New York (1996).
8. J. McHardy and S. Sawan, "Supercritical Fluid Cleaning," Noyes, Park Ridge, in press.
9. J. Jonas, Ed., "High Pressure NMR," NMR Basic Principles and Progress, Vol. 24, Springer-Verlag, Berlin (1991).
10. A. Abragam, "The Principles of Nuclear Magnetism," Clarendon, Oxford (1961).
11. C. D. Jeffries, "Dynamic Nuclear Orientation," Wiley, New York (1963).
12. K. H. Hausser and D. Stehlik, Dynamic nuclear polarization in liquids, *Adv. Magn. Reson.* **3,** 79–139 (1968).
13. M. Goldman, "Spin Temperature and NMR in Solids," Clarendon, Oxford (1970).
14. J. Trommel, "Molecular Motions and Collisions in Organic Free Radical Solutions as Studied by Dynamic Nuclear Polarization," Thesis, Delft University of Technology, Delft (1978).
15. A. Abragam and M. Goldman, "Nuclear Magnetism: Order and Disorder," Clarendon, Oxford (1982).
16. W. Müller-Warmuth and K. Meise-Gresch, Molecular motions and interactions as studied by dynamic nuclear polarization in free radical solutions, *Adv. Magn. Reson.* **11,** 1–45 (1983).
17. R. A. Wind, F. E. Anthonio, M. J. Duijvestijn, J. Smidt, J. Trommel, and G. M. C. de Vette, Experimental setup for enhanced ^{13}C NMR spectroscopy in solids using dynamic nuclear polarization, *J. Magn. Reson.* **52,** 424–434 (1983).
18. R. A. Wind, M. J. Duijvestijn, C. van der Lugt, A. Manenschijn, and J. Vriend, Applications of dynamic nuclear polarization in ^{13}C NMR in solids, *Prog. NMR Spectrosc.* **17,** 33–67 (1985).
19. M. J. Duijvestijn, R. A. Wind, and J. Smidt, A quantitative investigation of the dynamic nuclear polarization effect by fixed paramagnetic centra of abundant and rare spins in solids at room temperature, *Physica B* **138,** 147–170 (1986).
20. R. D. Bates, Dynamic nuclear polarization, *Magn. Reson. Rev.* **16,** 237–291 (1993).
21. R. A. Wind, Dynamic nuclear polarization and high-resolution NMR of solids, *Encyclopedia Magn. Reson.* **3,** 1798–1807 (1996).
22. A. W. Overhauser, Polarization of nuclei in metals, *Phys. Rev.* **92,** 411–415 (1953).
23. Y. Ayant, E. Belorizky, P. Fries, and J. Rosset, Effet des interactions dipolaires magnétique intermoléculaires sur la relaxation nucléaire de molecules plyatomiques dans les liquides, *J. Phys.* **38,** 325–337 (1977).
24. B. M. Odintsov, R. L. Belford, P. J. Ceroke, A. B. Odintsov, and R. B. Clarkson, Temperature dependence of solid-liquid scalar interactions in aqueous char suspensions by nonstationary DNP at low magnetic field, *Surf. Sci.* **393,** 162–170 (1997).
25. B. M. Odintsov, R. L. Belford, P. J. Ceroke, and R. B. Clarkson, Solid–liquid electron density transfer in aqueous char suspensions by ^{1}H-pulsed dynamic nuclear polarization at low magnetic field, *J. Am. Chem. Soc.* **120,** 1076–1077 (1998).
26. B. M. Odintsov, R. L. Belford, P. J. Ceroke, Z. Sh. Idiyatullin, R. S. Kashaev, I. V. Kuriashkin, V. S. Rukhlov, A. N. Temnikov, and R. B. Clarkson, Molecular diffusion and DNP enhancement in aqueous char suspensions, *J. Magn. Reson.* **135,** 435–443 (1998).
27. J. Jonas and D. M. Lamb, Transport and intermolecular interactions in compressed supercritical fluids, (*1,* pp. 15–28).
28. H. C. Dorn, T. E. Glass, L. Allen, R. Gitti, C. Tsao, C. Wild, and C. S. Yannoni, Flow NMR and DNP studies of dense fluids," presented at the 29th Experimental and NMR Spectroscopy Conference, Rochester, New York (1988).
29. H. C. Dorn, R. Gitti, K. H. Tsai, and T. E. Glass, The flow transfer of a bolus with ^{1}H dynamic nuclear polarization from low to high magnetic fields, *Chem. Phys. Lett.* **155,** 227–232 (1989).
30. H. C. Dorn, T. E. Glass, R. Gitti, and K. H. Tsai, Transfer of ^{1}H and ^{13}C dynamic nuclear polarization from immobilized nitroxide radicals to flowing liquids, *Appl. Magn. Reson.* **2,** 9–27 (1991).
31. M. Afeworki, R. A. McKay, and J. Schaefer, Selective observation of the interface of heterogeneous polycarbonate/polystyrene blends by dynamic nuclear polarization carbon-13 NMR spectroscopy, *Macromol.* **25,** 4084–4091 (1992).
32. C. R. Yonker, T. S. Zemanian, S. L. Wallen, J. C. Linehan, and J. A. Franz, A new apparatus for the convenient measurement of NMR spectra in high-pressure liquids, *J. Magn. Reson. A* **113,** 102–107 (1995).
33. S. Bai, G. Taylor, C. L. Mayne, R. J. Pugmire, and D. M. Grant, A new high pressure sapphire nuclear magnetic resonance cell, *Rev. Sci. Instrum.* **67,** 240–243 (1996).
34. "Gas Encyclopedia," Elsevier/North-Holland, New York (1976).
35. R. A. Wind, L. Li, G. E. Maciel, and J. B. Wooten, Characterization of electron spin exchange interactions in cellulose chars by means of ESR, ^{1}H NMR, and dynamic nuclear polarization, *J. Appl. Magn. Reson.* **5,** 161–168 (1993).
36. J. J. Krebs, Proton spin polarization of water adsorbed on sucrose chars, *J. Chem. Phys.* **34,** 326–329 (1961).